Feasibility analysis of smartphone GNSS data for low-frequency cm-level motion monitoring

Chenyu XUE[1], **Guangcai LI**[2,3], **Jianghui GENG**[2,3], and **Panos PSIMOULIS**[1,*]

[1] *Nottingham Geospatial Institute, Nottingham, UK. (Chenyu.Xue@notitngham.ac.uk) (Panagoitis.Psimoulis@nottingham.ac.uk)*

[2] *GNSS Research Center, Wuhan University, Wuhan, China. (guangcai.li@whu.edu.cn) (jgeng@whu.edu.cn)*

[3] *Innovation Academy for Precision Measurement Science and Technology, Chinese Academy of Sciences, Wuhan, China.*

[*] *corresponding author*

Abstract

In the last few years, to get better positioning performance, smartphone industry has developed mobile phones capable of dual frequency carrier phase measurements, leading to many well-known globally manufacturers incorporating this feature in their latest models. Although expectedly noisy Global Navigation Satellite System (GNSS) measurements due to the linearly polarised smartphone GNSS antenna and chipset GNSS receiver, the dual frequency carrier phase plus GPS, Galileo, GLONASS, Beidou (BDS) multi-constellation observation capabilities have made them potential candidates for precise location and positioning applications. In this paper, we aim to explore the feasibility of these smartphone antenna/receiver in monitoring low-frequency periodic cm-level motion, for evaluating the possibility of employing them in structural health monitoring related applications. We have conducted two controlled oscillation displacement experiments in the lab with mobile phones for displacement detection. It was found that motions as small as 2-cm amplitude and frequencies as low as 0.05 Hz could be monitored, with an accuracy of 5-8 mm from displacement measurement, and a maximum 6% deviation from dominant frequency derivation, respectively.

Keywords: Smartphone, GNSS, deformation monitoring

Received: 9th December 2024. Revised: 26th February 2025. Accepted: 15th March 2025.

1 Introduction

Since the start of era of smartphone in 2000s, smartphones are becoming increasingly common and prevalent in many engineering and positioning/navigation applications. Until recent years, for better positioning performance, smartphones capable of dual frequency carrier phase measurements are released; with the first smartphone, Xiaomi Mi 8 (released in 2018) supporting dual frequency GPS/Galileo, single frequency BDS/GLONASS code pseudo-range and carrier phase measurements (Robustelli et al., 2019, Geng and Li, 2019). Nowadays, with the development of more advanced mobile phone chipsets, several smartphone manufacturers are releasing flagship phones supporting features such as L1/E1, L5/E5a dual frequency, multi-GNSS carrier phase measurements capability, etc. Thanks to GPSTest mobile app developed by Barbeau (2023), the capability of recent smartphones as of GNSS performance are crowdsourced and documented in GPSTest database (Barbeau, 2021).

Research studies were conducted after the release of the first dual-frequency GNSS carrier phase Mi8. Robustelli et al. (2019) used Xiaomi Mi8 in both single point positioning (SPP) and post-processing kinematic (PPK) applications, showing an RMS accuracy of around 5 m and 1-2 m for the SPP and PPK, respectively. Chen et al. (2019) employed Xiaomi Mi8 for real time precise point positioning and found that the RMS positioning error is 0.81 m and 1.65 m for horizontal and vertical respectively.

Since then, researchers have assessed the GNSS performance of various smartphones. Paziewski et al. (2021) assessed the GNSS observation quality using several smartphones and concluded that the code and phase measurement errors are evidently larger compared to geodetic GNSS receivers, but still feasible to obtain a cm-level static solution. Li and Geng (2019) analysed GNSS measurement error characteristics from Nexus 9 tablets using both embedded and external antennas, revealing that the root mean squared (RMS) accuracy for the SPP is about 10-20 m, and cm-level precision can be achieved for static PPK solutions.

It seems promising that cm-level of precision using mobile phone could be achieved based on various research using relative PPK positioning (Pesyna et al., 2014; Wanninger and Heßelbarth, 2020; Geng and Li, 2019; Dabove and Pietra, 2019). However, most of the experiments are based on static experiments and only one study is based on experiments of dynamic motion of smartphone experiments (Vazquez-Ontiveros, et al., 2024).

With the broader trend of applying low-cost GNSS receivers for monitoring applications (Xue et al., 2021; Xue et al., 2022; Xue and Psimoulis, 2023), there is great potential for mobile phones to be used for precise positioning services such as in SHM due to: 1) being a relatively low-cost alternative of geodetic receiver, 2) the option of disabling the duty cycle in recent smartphone models, resulting to continuous GNSS measurement, 3) the raw smartphone GNSS measurements (code and carrier phase, etc.) which are accessible to the broader smartphone users community, 4) the potential of crowdsourcing data through the smartphones application, and 5) availability of various sensors such as accelerometers, gyros, which can be combined with GNSS measurements in SHM applications (Lăpădat et al., 2021).

In general, it is expected that the code and carrier phase measurements of smartphones are of relatively lower quality than those of geodetic receiver. However, Wanninger and Heßelbarth (2020) showed that ambiguity resolution of L1 measurements can be achieved for GPS measurements by using a Huawei P30. It is promising to say that the integer ambiguity fix could be achieved for GPS L1, as the ambiguity fix is the prerequisite for achieving a more precise solution down to cm level.

Although there are a few studies regarding deformation monitoring with smartphones, most of them, only take advantage of its embedded accelerometer, their GNSS observation functionality is rarely assessed for its deformation monitoring applicability except for few conducted by Zeng et al., (2022) and Vazquez-Ontiveros et al. (2023). Vazquez-Ontiveros et al. (2023) found that an RMS error of 1.4 cm in the horizontal component could be achieved for kinematic circular trajectory with a rotating speed of 0.44 rad/s (~0.07 Hz) and an rotation radius (amplitude) of 19 cm and RMS errors of 0.7 cm, 1.2 cm, and 4.2 cm in the East, North, and Up components could be obtained with static experiment.

In this contribution, we explore the feasibility of smartphone GNSS in monitoring relative dynamic displacements. Below, we present preliminary results of smartphone GNSS data in controlled experiments of dynamic low-frequency motion, evaluating its potential for SHM applications for flexible structures.

2 Methodology

We conducted two kinematic experiments to simulate long-period (up to 0.2 Hz) cm-level or larger motion, meeting the main deflection characteristics (amplitude and frequency) of flexible structures (e.g., long bridges and tall buildings) under normal service conditions (Meng et al., 2018;).

The first experiment involved a controlled vertical periodic motion (of up to 0.1 Hz) produced manually by a platform, following the methodology of the study Peppa et al. 2018, and monitored by smartphone GNSS receiver and a robotic total station (RTS) measurements. The mm-level accuracy of RTS measurements served as the reference to evaluate the performance of the smartphone GNSS (Psimoulis et al., 2008).

The second experiment focused on controlled horizontal oscillations of up to 0.2 Hz, induced by a shake table. Multiple GNSS sensors, such as survey-grade , low-cost and smartphone-grade receivers, were attached to the shake table, along with several accelerometers, all subjected to the same excitations. The direct trajectory output of the shake table was used as a reference to assess the performance of different sensors. Similar timeseries/residuals and spectral analyses are conducted in both experiments to quantify measurement accuracy and identify their dominant frequencies.

3 Controlled vertical experiment

The first experimental assessment aimed to evaluate the performance of GNSS-smartphone for monitoring low frequency cm-level vertical dynamic motion. We conducted an experiment on the open roof of Nottingham Geospatial Building (NGB), where periodic vertical oscillations were executed by using a heavy-duty tripod with a height-adjustable platform and manually controlled vertical movement. On the top of the tripod, a 360o-prism and metallic plate were mounted, where the smartphone was securely placed. We manually introduced vertical periodic oscillations of about 0.05 Hz and 0.1 Hz by synchronising to a metronome, as described in Peppa et al., 2018, and the amplitude of 2 to 3 cm was controlled based on the graduation etched on the pole.

The setup of the vertical controlled experiment is shown in Figure 1, where the GNSS base station is consisted of Leica AS10 geodetic antenna and Leica GS10 geodetic receiver, recording in 1 Hz multi-GNSS observations (i.e. GPS, GLONASS, Galileo, BDS; Figure 1A). The Samsung S23 FE, was used as GNSS rover placed on top of a ground plate for multipath suppression, recording 1Hz multi-GNSS observations, using the GnssLogger App, developed by Google (Google, 2024). The Samsung S23 FE could record L1/L5 GPS, B1i/B2a BDS, E1/E5a Galileo, and G1 GLONASS signals. Finally, the 360º-prism Leica prism was monitored by Leica TS30 RTS, which was recording at 10 Hz sampling-rate (Peppa et al., 2018, Peppa and Psimoulis, 2023).

Figure 1. (left) The GNSS base station, (middle) the rover station with the prism and a metallic plate where the Samsung S23 FE has been mounted, and (left) the RTS recording the position of the prism.

We conducted a total of six oscillations; (i) three oscillations of approximately 0.1 Hz frequency, and amplitude of ~2 cm (A) and ~3cm (B and C); and (ii) three oscillations of approximately 0.05 Hz frequency and amplitude of ~2 cm (D) and ~3 cm (E and F).

The RTS ortho-height timeseries relative to the initial position (prior to the oscillation) were exported, expressing the vertical displacement of the oscillation. The smartphone GNSS data were logged in Receiver Independent Exchange Format (RINEX) 3.03 from the GnssLogger App. The GNSS data were post-processed using double-difference (DD) in kinematic mode in RTKLIB demo5 b34h (Everett, 2023) with mobile GNSS data as the rover and Leica GS10 data as the base. The multi-GNSS solutions were obtained using GPS, Galileo and BDS observations. The GLONASS observations were excluded due to the GLONASS inter-frequency bias and ambiguity resolution (Msaewe et al., 2017). The Up-component time-series of the GNSS solution reflected the vertical oscillation and was compared against the RTS vertical timeseries to evaluate the accuracy of the GNSS smartphone data.

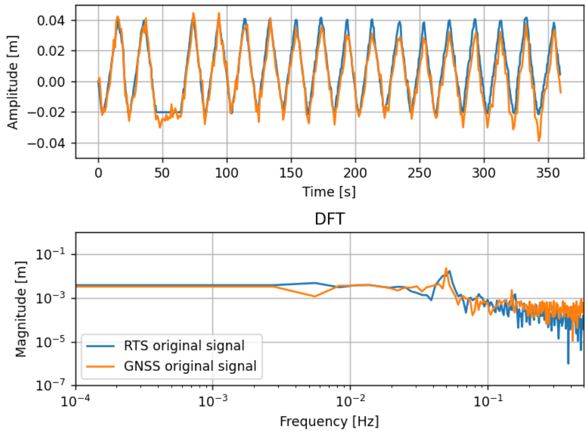

Figure 2. (top) RTS and GNSS-smartphone timeseries for case F oscillation case, and (bottom) the respective speactra

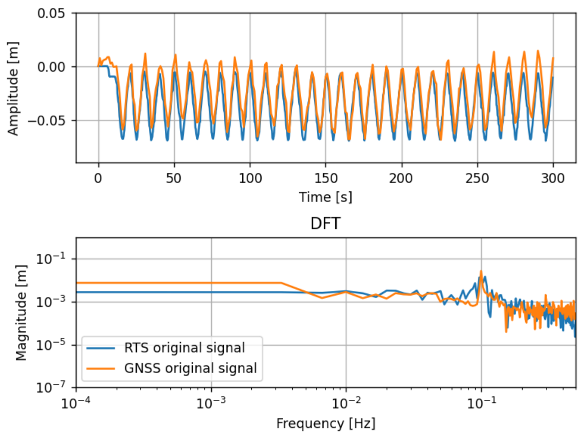

Figure 3. (top) RTS and GNSS-smartphone timeseries for the case C oscillation case, and (bottom) the respective DFT spectra

Figure 2 shows the vertical component timeseries and Discrete Fourier Transform (DFT) spectra of the RTS and GNSS data for the oscillation case of ~0.05 Hz frequency and ~3cm amplitude (case F) respectively. It is clearly observed a pattern of sinusoidal movement in the timeseries, with a slight downward drift observed in the GNSS time-series, which might be due to multipath effect to which is susceptible the the linearly polarised smartphone antenna.

Likewise, in Figure 3 are presented the Up-component time-series and the respective spectra of GNSS and RTS data for case C (amplitude of ~3cm, frequency of ~0.1 Hz). Similarly, a consistent vertical oscillation is observed in RTS time-series, whereas a long period pattern is observed in the smartphone GNSS time-series, probably due to the multipath. However, the spectra of both RTS and GNSS reveal the dominant frequency of frequency of 0.1Hz.

To quantify the precision of the smartphone GNSS measurement, the residuals between smartphone GNSS timeseries and RTS were computed after they were resampled to the same frequency of 10 Hz and finally synchronised by cross-correlating the time-series. The residual time-series expressed a main periodic pattern similar to that of the motion frequency, which is due to potential phase shift between the resampled GNSS and RTS time-series. Even though the periodic pattern of the residuals, the standard deviations of the residuals for each oscillation scenario was computed as an indication of the obtainable precision of the smartphone GNSS.

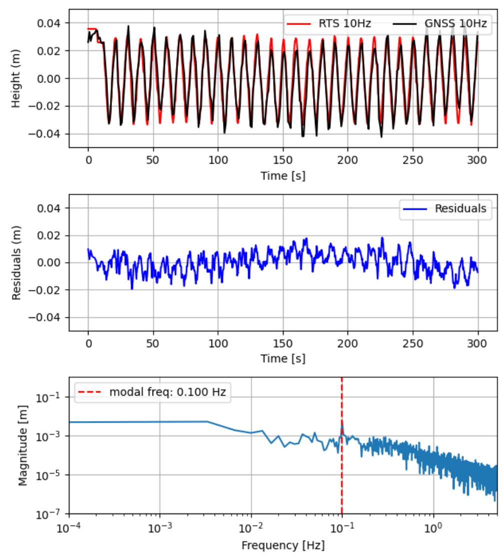

Figure 4. (top) The RTS and the GNSS-smartphone original timeseries after resampled to 10Hz for case C oscillation, (middle) the residuals computed by the difference between the 10Hz RTS and GNSS time, and (bottom) the residuals DFT spectrum.

Table 1 shows the dominant frequency detected for each oscillation scenario derived from the analysis of the RTS and the smartphone GNSS time-series, and corresponding precision calculated based on the standard deviation of the residuals derived after the subtraction of the GNSS timeseries from the RTS timeseries. It is observed that the GNSS-smartphone precision ranges 5-8 mm, expressing though the difference between GNSS and RTS data due to the phase shift. As for the dominant frequency derivation, the maximum discrepancy between smartphone GNSS and RTS is around 0.007 Hz for 0.1 Hz detection, and 0.003Hz for 0.05Hz detection, equivalent to 6-7% bias in dominant frequency determination. It is also interesting to note that the spectra for RTS timeseries doesn't seem to have distinct peaks but rather shows an area of occurrence of multiple peaks as compared to the smartphone GNSS, indicating that it is more sensitive in differentiating different frequencies in the signal. Finally, the DFT of residuals also shows periodic pattern (Figure 4).

Table 1. Precision of the smartphone GNSS in monitoring the kinematic oscillatory displacement for scenarios A to F, and the corresponding dominant frequency from RTS and smartphone GNSS for each case

	Precision (mm)	**Freq (Hz)**	
	Original GNSS timeseries	**Freq (RTS)**	**Freq (GNSS)**
A	5.1	0.100	0.100
B	5.5	0.100	0.094
C	7.1	0.107	0.100
D	4.6	0.050	0.050
E	4.2	0.050	0.050
F	4.7	0.053	0.050

4 Controlled horizontal experiment

The experiments of horizontal dynamic motion was based on a shake table and it was designed and conducted on the roof of Xinghu Experimental Building at Wuhan University in China. The roof is moderately open with few obstructions by surrounding buildings.

In Figure 5 is presented the experimental setup, where several mobile phones were placed on top of a shake table device, (i) with two smartphones placed outside using their internal GNSS antenna (Huawei P40 and Samsung S23 FE), (ii) two mobile phones placed inside of two shielding boxes (Huawei P40 in the black box and Samsung S23 PE in the white box). The two shielding boxes and the geodetic receiver were both connected to the survey grade antenna via a signal splitter. Inside the two shielding boxes, there were two devices retransmitting the GNSS signal as received by the GNSS geodetic antenna to the smartphone. A patch antenna was also placed on the white shielding box connecting to a ublox F9P module, and a survey-grade accelerometer was fixed on the side of the shake table.

Figure 5. (left) The setup of the rover sensors (GNSS and accelerometer) on the shake table, and (right) the station consisted of survey-grade antenna and receiver

Both the geodetic rover and base station were measuring at a sampling rate of 10 Hz, recording GPS, Galileo, BDS, GLONASS and QZSS observations, while all four smartphones were configured so that the GPS (L1/L5), Galileo (E1/E5a), GLONASS (G1), QZSS (J1/J5), and BDS (B1i/B2a) GNSS raw data were recorded with application GeoDataLogger developed by PrideLab (2024) at a sampling frequency of 1Hz. Additionally, the u-blox receiver was recording GPS, Galileo, GLONASS), QZSS and BDS observations at 10Hz sampling rate.

The accelerometer data were also recorded in GeoDataLogger at the maximum capacity of the smartphone (e.g., around 125 Hz sampling frequency for Samsung and around 100Hz for the rest), while the survey grade accelerometer (TD) recorded at 100 Hz sampling frequency with GPS timestamp thanks to an external GNSS module.

The Quanser Shake Table II, controlled via a MATLAB script implemented in Simulink, was used to perform precise, programmed displacements. The shake table was rigidly bolted to the roof and carefully orientated in E-W direction. We performed in total 25 different motions with various amplitude and oscillating frequency oscillating in E/W direction, with amplitude ranging from 5mm, 10mm, 20mm, 40mm, and oscillation frequency ranging from 0.1 Hz, 0.2Hz, 0.5Hz, 1Hz, 1.5Hz, and 2Hz. Each oscillation lapsed around 2 minutes with at least 1 minute of static period in between consecutive oscillations. Thanks to the MATLAB, the shake table could output direct displacement timeseries at a frequency of 100 Hz, which we employed as the reference data as the ground truth.

It is worth noting that from the experiment,

i) Apart from the GNSS measurements and the geodetic accelerometer data, all other data was not initially synchronised to GNSS time, such as phone accelerometer measurement and shake table output timeseries.

ii) The acceleration timeseries derived directly from the accelerometers output, with the oscillation axis being in East-West direction. The acceleration data of the smartphones were acquired depending on the orientation of each smartphone.

iii) The smartphones can record 1Hz GNSS measurements, meaning that they can be used only for frequencies up to 0.5Hz, due to Nyquist theorem

iv) The ublox measurement terminated halfway during the measurement, causing some data loss.

The GNSS data is postprocessed using the open-source software RTKLIB demo5 b34k (Everett, 2024) in the kinematic mode, with the GNSS sensors on the shake table as rover and the geodetic receiver as base forming multiple baselines. The output from the RTKLIB is in E/N/U which is effectively the 3D projection of the baseline vector in the local E/N/U direction. All the postprocessed solutions achieved ambiguity fix.

The synchronisation of the accelerometer and GNSS timeseries, is based on finding and shifting the optimum lag when the cross correlation between the geodetic accelerometer and each accelerometer timeseries reached the maximum, indicating strong correlation. By adjusting the time for accelerometer timeseries, we aligned them to GNSS timestamps.

In this study, we focused only on oscillations with frequency motion up to 0.2 Hz, for which the 1 Hz smartphone GNSS data can be used to determine the oscillation frequency. For higher frequencies, the 1-Hz GNSS smartphone data would need to be integrated with accelerometers data. Hence, we investigate only the performance of the 1-Hz GNSS data.

The RTKLIB setting for processing GNSS timeseries are utilising L1+L2/E5b+L5/E5a triple frequency option and GPS+Galileo+BDS multi-constellation configuration. Slightly different configuration settings were used for phones using internal antenna and the geodetic antenna due to the significant differences in the antenna since mobile phones antenna is more susceptible to multipath error, cycle slips.

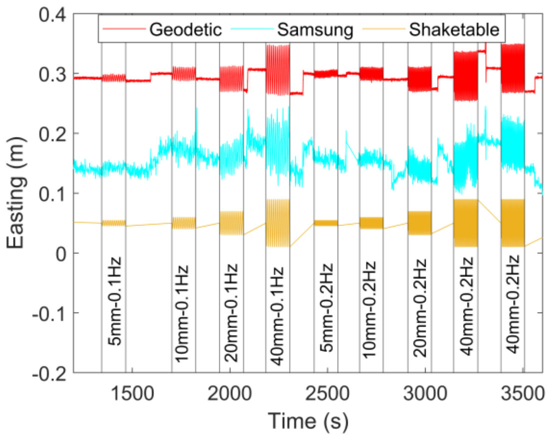

Figure 6. Original timeseries from different GNSS sensors. From top to bottom are 1) geodetic receiver/antenna, 2) Samsung S23 FE 3) output from shake table. The time-series are shifted to avoid overlap between them.

In Figure 6, it is shown the timeseries from different monitoring sensors installed on the shake table for oscillations with frequency less than 0.5 Hz, which is the Nyquist frequency for the smartphone sampling rate. The start and end time for each oscillation is highlighted in Figure 6 by two vertical lines segmenting the timeseries into 9 oscillation sections. The oscillation characteristics (amplitude and oscillation frequency) for the 9 sections from left to right are shown in the Table 2.

It can be shown in Figure 6 that the geodetic receivers with geodetic antenna time series doesn't seem to be affected by low frequency errors as much as the Samsung timeseries. Andhe noise level is significantly larger for Samsung as compared to geodetic receiver/antenna when the shake table was static. These might imply that the antenna grade is crucial for a more precise results less affected by multipath. On the other hand, it is promising that the displacement/excitations could be detected from Samsung timeseries with a strong positive correlation with the geodetic GNSS and shake table timeseries, especially for 20- and 40-mm amplitude oscillations.

Table 2. Characteristics (Amplitude and Frequency) of different oscillations

Oscillation	Amplitude (mm)	Frequency (Hz)
1	5	0.1
2	10	0.1
3	20	0.1
4	40	0.1
5	5	0.2
6	10	0.2
7	20	0.2
8	40	0.2
9	40	0.2

To gauge the accuracy of the GNSS measurement, the GNSS timeseries was firstly filtered using high-pass Chebyshev filter with cutoff frequency of 0.05 Hz to mitigate the multipath bias. Then, the residuals were calculated by the difference between the GNSS timeseries and the output from shake table. The standard deviation is calculated for the residuals and is shown in the Table 3.

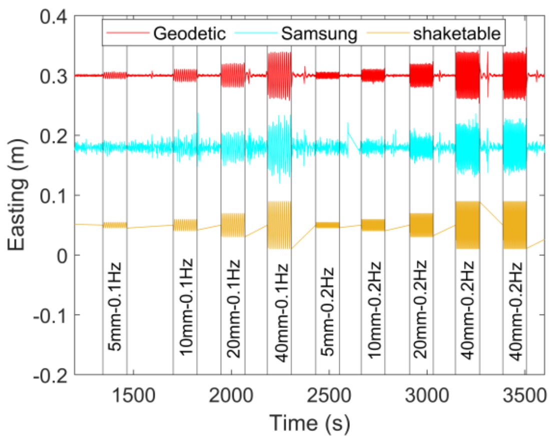

Figure 7. Similar to Figure 6, timeseries from different GNSS sensors but after high-pass filter

It is shown in Table 3 that geodetic receiver/antenna has a precision of below ~3 mm, and the precision from Samsung smartphone is in the range of 3-8 mm, more than twice as worse as the geodetic solution. The overall worse performance is as expected from mobile phone since the geodetic receiver/antenna are dedicated GNSS instruments, whereas the mobile phones has comparatively lower grade receiver and antenna.

Table 3 also suggests that smartphone on its own, to be more specific, without external antenna, without accelerometer coupling, are probably not the best option for monitoring 5 mm, and 10 mm displacements due to worse precisions, i.e. 4-7 mm precision as compared to the amplitude being monitored, which could also be concluded from Figure 6 and 7. On the other hand, for oscillation cases with amplitude of 20 mm and 40 mm, the precisions for Samsung smartphone maintain around 4-8 mm, indicating its potential for monitoring those displacements.

Table 3. Standard deviation of the residuals for different GNSS sensors with reference to Shake table timeseries

Oscillation	Standard deviation (mm)	
	Geodetic	**Samsung**
1	0.7	3.7
2	0.9	7.0
3	1.5	4.6
4	3.2	7.8
5	0.8	4.9
6	1.2	4.1
7	1.6	4.1
8	2.3	5.9
9	2.9	4.6

Table 4. Dominant frequency derived from each sensor, the percentages in brackets indicate the deviation in percentage from the reference dominant frequency derived from DFT of shake table timeseries.

	Frequency (Hz)		
	Geodetic	**Samsung**	**Shake table**
1	0.098 (2%)	0.098 (2%)	0.096
2	0.099 (2%)	0.098 (1%)	0.097
3	0.098 (2%)	0.098 (2%)	0.096
4	0.098 (2%)	0.098 (2%)	0.096
5	0.197 (-2%)	0.197 (-2%)	0.202
6	0.200 (-1%)	0.203 (0%)	0.203
7	0.197 (-3%)	0.203 (0%)	0.203
8	0.197 (-3%)	0.203 (0%)	0.203
9	0.202 (2%)	0.200 (1%)	0.199

Similarly, we conducted DFT for the original timeseries. The frequency that can be detected from the original timeseries is shown in Table 4.

It could be seen from Table 4, the dominant frequency could be derived from mobile phone with deviation no more than 2-3% from the reference frequency derived from shake table output timeseries. Especially for with Samsung mobile phone, although the waveform from the timeseries seems very ambiguous especially for low amplitude oscillations (e.g. 5mm, 10mm), the dominant frequency for the oscillation could still be retrieved.

5 Conclusion

In this contribution, we analysed the performance of smartphones in monitoring vertical and horizontal oscillations with controlled oscillation setups, particularly for low frequency and low amplitude displacement, with frequency less than or equal to 0.5 Hz, and amplitude less than 4 cm.

Thanks to smartphones L1/L5, E1/E5a, dual frequency, carrier phase measuring capability, in the vertical controlled experiment, it is concluded that amplitude of 2-3 cm and frequency of 0.05-0.1 Hz could be very accurately determined with reference to RTS measurement, with a precision of 5-8mm and a deviation of 6% in frequency determination. On the other hand, for the controlled horizontal oscillation experiment, it is concluded that smartphone could achieve 4-8 mm precision in 0.1 Hz and 0.2 Hz oscillation experiments, with a maximum 3% deviation for frequency determination.

However, due to 1 Hz sampling rate from the mobile phone, the oscillation above 0.5 Hz could not be detected due to aliasing. Therefore, the future plans it to (i) investigate the sensor fusion between high frequency accelerometer measurement and GNSS measurement for detection of higher frequency displacement, and (ii) the application of GNSS smartphone in real structural monitoring projects, examining the performance of GNSS smartphone in real monitoring conditions.

Acknowledgements

This work is funded by Royal Society International Exchange Collaboration grant with National Natural Science Foundation of China (IEC\NSFC\223184)

References

Barbeau, S. (2021). Crowdsourcing GNSS features of Android devices. https://bit.ly/gpstest-device-database

Barbeau, S. (2023). GPSTest. [Mobile app] Google play store. Available at https://play.google.com/store/apps/details?id=com.android.gpstest&hl=en_GB

Chen, B., Gao, C., Liu, Y., & Sun, P. (2019). Real-time precise point positioning with a Xiaomi MI 8 android smartphone. *Sensors*, *19*(12), 2835.

Dabove, P., & Di Pietra, V. (2019). Towards high accuracy GNSS real-time positioning with smartphones. *Advances in Space Research*, *63*(1), 94-102.

Everett, T. (2023). RTKLIB: demo5 b34h. Accessed December 05, 2024. https://github.com/rtklibexplorer/RTKLIB/releases/.

Everett, T. (2024). RTKLIB: demo5 b34k. Accessed December 05, 2024. https://github.com/rtklibexplorer/RTKLIB/releases/.

Geng, J., & Li, G. (2019). On the feasibility of resolving Android GNSS carrier-phase ambiguities. *Journal of Geodesy*, *93*(12), 2621-2635.

Google. (2024). GnssLogger App. [Mobile app] Google play store. Available at https://play.google.com/store/apps/details?id=com.google.android.apps.location.gps.gnsslogger&hl=en_GB

Li, G., & Geng, J. (2019). Characteristics of raw multi-GNSS measurement error from Google Android smart devices. *GPS solutions*, *23*(3), 90.

Msaewe, H. A., Hancock, C. M., Psimoulis, P. A., Roberts, G. W., Bonenberg, L., & de Ligt, H. (2017). Investigating multi-GNSS performance in the UK and China based on a zero-baseline measurement approach. *Measurement*, *102*, 186-199.

Paziewski, J., Fortunato, M., Mazzoni, A., & Odolinski, R. (2021). An analysis of multi-GNSS observations tracked by recent Android smartphones and smartphone-only relative positioning results. *Measurement*, *175*, 109162.

Peppa, I., & Psimoulis, P. A. (2023). Detection of GNSS antenna oscillatory motion and multipath conditions via exploitation of multipath-induced SNR variations. *GPS Solutions*, *27*(3), 117.

Peppa, I., Psimoulis, P., & Meng, X. (2018). Using the signal-to-noise ratio of GPS records to detect motion of structures. *Structural control and health monitoring*, *25*(2), e2080.

Pesyna, K. M., Heath, R. W., & Humphreys, T. E. (2014, September). Centimeter positioning with a smartphone-quality GNSS antenna. In *Proceedings of the 27th International Technical Meeting of the Satellite Division of The Institute of Navigation (ION GNSS+ 2014)* (pp. 1568-1577).

PrideLab. (2024). Smartphone multi-frequency GNSS and IMU data acquisition. available at https://github.com/PrideLab/PRIDE-GeoDataLogger/tree/main

Robustelli, U., Baiocchi, V., & Pugliano, G. (2019). Assessment of dual frequency GNSS observations from a Xiaomi Mi 8 Android smartphone and positioning performance analysis. Electronics, 8(1), 91.

Vazquez-Ontiveros, J. R., Martinez-Felix, C. A., Melgarejo-Morales, A., Retegui-Schiettekatte, L., Vazquez-Becerra, G. E., & Gaxiola-Camacho, J. R. (2024). Assessing the quality of raw GNSS observations and 3D positioning performance using the Xiaomi Mi 8 dual-frequency smartphone in Northwest Mexico. *Earth Science Informatics*, *17*(1), 21-35.

Wanninger, L., & Heßelbarth, A. (2020). GNSS code and carrier phase observations of a Huawei P30 smartphone: Quality assessment and centimeter-accurate positioning. *GPS Solutions*, *24*(2), 64.

Xue, C., & Psimoulis, P. A. (2023). Monitoring the dynamic response of a pedestrian bridge by using low-cost GNSS receivers. *Engineering Structures*, *284*, 115993.

Xue, C., Psimoulis, P. A., & Meng, X. (2022). Feasibility analysis of the performance of low-cost GNSS receivers in monitoring dynamic motion. *Measurement*, *202*, 111819.

Xue, C., Psimoulis, P., Zhang, Q., & Meng, X. (2021). Analysis of the performance of closely spaced low-cost multi-GNSS receivers. *Applied Geomatics*, *13*(3), 415-435.